An approach towards understanding mode II failure of poly(methyl methacrylate)

F. Ramsteiner
Kunststofflaboratorium, Abt. Polymerphysik, Festkörperphysik, BASF Aktiengesellschaft, D-6700 Ludwigshafen, Germany
(Received 24 July 1991; revised 20 March 1992)

In order to evaluate the mode II sliding failure in poly(methyl methacrylate) (PMMA), various types of specimens have been tested. Without side grooves in the specimens, the polymer fails when macroscopically sheared generally by an off-plane crack with the crack opening behaviour of mode I. With side grooves along the shear plane, the matrix shear strength dominates failure, and real mode II sliding failure was not attainable. In uniaxially reinforced composites, shear failure is enforced in the matrix by the fibres, which prevent the matrix from opening in an off-plane direction.

(Keywords: failure; poly(methyl methacrylate); mechanical properties)

INTRODUCTION

Fracture mechanics is becoming a very useful instrument for characterizing the failure of materials, since this method, in contrast to most other standards, describes real material properties, independent of specimen geometry. This objective is attained by concentrating on the stress intensity at the tip of a macroscopic notch, the instability of which and the following crack propagation are quantified. One of the final aims of this method must be to find a three-dimensional failure criterion that allows one to reduce an actual deformation state near the crack to the three principal critical modes of deformation: namely, mode I, which is active by crack opening; mode II, describing sliding or shearing in the direction of the notch; and mode III, characterizing the tearing behaviour perpendicular to the notch direction. An additional reason for measuring mode II failure of a polymer is to improve the understanding of the role that such material plays as a matrix in fibre-reinforced composites. Whereas in polymers mode I measurements are widely applied, the sliding mode II reveals some difficulties from an experimental as well as from a theoretical point of view. This special problem in respect of evaluating the sliding mode II will be discussed in this paper.

For this study poly(methyl methacrylate) (PMMA) was used to be able to observe visually crack instability.

PROBLEM

If, for example, a CT specimen is macroscopically sheared along the plane of the notch, according to the mode II condition a crack starts at the tip of the notch in a direction oblique to the plane of expected shear (*Figure 1*), and no shearing occurs. This fracture behaviour has been described often in the literature[1–6] and is attributed to the statement that even in the macroscopic shear situation a crack develops:

(a) at the notch tip;

(b) in the direction perpendicular to the highest hoop stress, not along the plane of highest shear stress.

Discarding minor modifications[7], Erdogan and Sih[2] and others showed on the basis of the hoop stress, given near the notch tip by:

$$\sigma_\theta = \frac{1}{\sqrt{(2\pi r)}} \cos(\theta/2)[K_I \cos^2(\theta/2) - \tfrac{3}{2} K_{II} \sin\theta] \quad (1)$$

(K = stress intensity factor for mode I and mode II; r, θ = cylindrical coordinates) that when shearing a crack, i.e. if

$$K_I = 0 \qquad K_{II} \neq 0 \quad (2)$$

the highest hoop stress operates in a plane about $\theta = -70°$ to the shear plane, and this is indeed often the direction of crack initiation at the tip of the notch. Therefore, from an engineering viewpoint, the failure criterion even for a mixed mode is expected to be mainly defined by the maximum hoop stress under the given stress–strain conditions. In other words, crack opening of mode I type dominates also mode II behaviour in isotropic materials. So it is not surprising that according to the literature K_{IIc} values are either very close to the K_{Ic} values, or often only slightly higher, probably due to friction effects between the planes of the notch in shearing and the slightly lower dilatational strain in the specimen under shear than under tensile stress. From a theoretical point of view[2] the maximum stress criterion claims that K_{IIc} should be even 15% lower than K_{Ic}.

The situation is totally different in fibre-reinforced composites, when stressed by mode II to evaluate interlaminar shear strength. In this case the propagating crack is obviously forced into the shear plane between the fibres. So the matrix between the fibres must shear. Hence, the shear properties of the matrix material in composites when measured in mode II cannot simply be derived from mode II measurements of the pure polymer, since the failure mechanism is different: in the composite a shearing mode operates; in the pure material a crack

0032-3861/93/020312-06

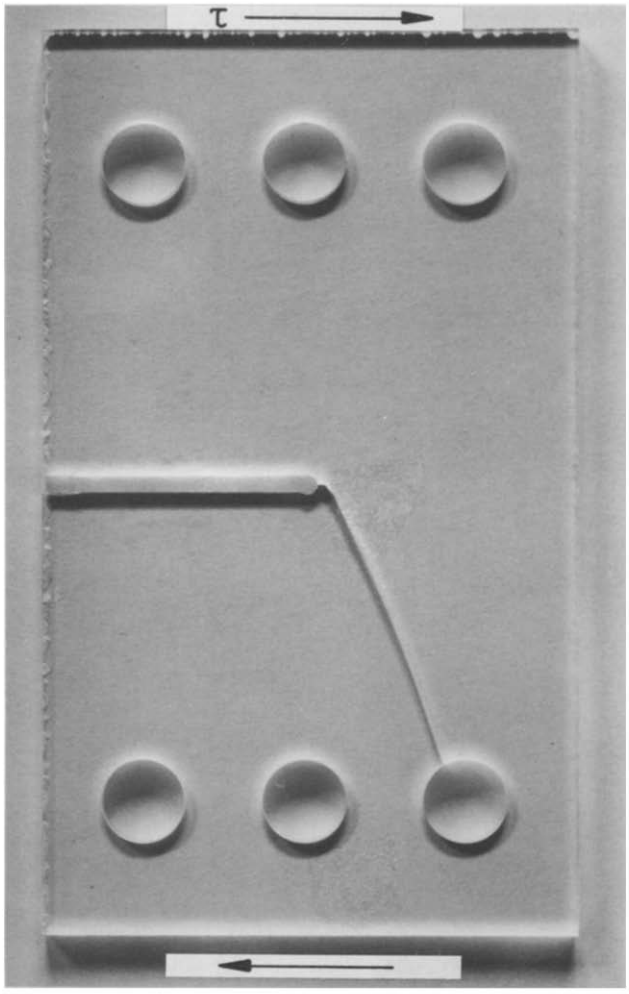

Figure 1 Sheared CT specimen, showing off-plane crack propagation

opening mode occurs. This shortcoming was also the motivation within the field of product development to look for specimens with guided crack propagation for measuring mode II shearing already in unreinforced materials.

EXPERIMENTS AND DISCUSSION

ELS specimen

As can be shown easily[8], ELS specimens have the advantage that the highest stress is concentrated near the crack tip, not only due to the stress intensity of crack tips, but also from the deformation line, leading to stable crack growth and not to catastrophic spontaneous crack propagation. As can be seen in *Figure 2a*, by deforming an ELS specimen of PMMA, the initial notch becomes unstable by crack initiation and propagation oblique to the shear plane. The above mentioned $-70°$ crack deviation is observed. The compliance $C(a)$ of this type of specimen can be measured as a function of crack length by increasing the length a of the notch in the direction of the shear plane by stepwise sawing. From this procedure follows:

$$C(\text{mm N}^{-1}) = 0.0073 + 1.25 \times 10^{-2}(a/L)^3 \quad (3)$$

By transferring these 0° compliance measurements in a very first approximation[9] to the observed $-70°$ crack instability, formal values for the energy release rate for mode II (G_{IIc}) are obtained for different initial crack lengths (*Table 1*). These calculations are based on the relationship:

$$G_{IIc} = \frac{P^2}{2B}\frac{dC}{da} \quad (4)$$

(P = force at fracture, B = thickness of the specimen at the fracture plane).

The notches have been sharpened by tapping a razor blade into the notch. The G_{IIc} values seem to be independent of crack length, as expected within the framework of fracture mechanics. In relation to the measured energy release rate for mode I:

$$G_{Ic} = 480 \text{ J m}^{-2}$$

the average value for mode II as obtained according to the procedure described above:

$$G_{IIc} = 440 \pm 40 \text{ J m}^{-2}$$

is comparable. These very similar values for both properties reveal obviously the same crack opening mechanism in both situations. Real shear failure must be much higher.

With the intention of forcing the crack to propagate by shear processes in the plane given by the initial notch, side grooves along the plane were milled on both sides of the specimen (*Figure 2b*). Now shear failure could be obtained; the deformation curves are non-linear. With the 5% offset values on the deformation curve and with

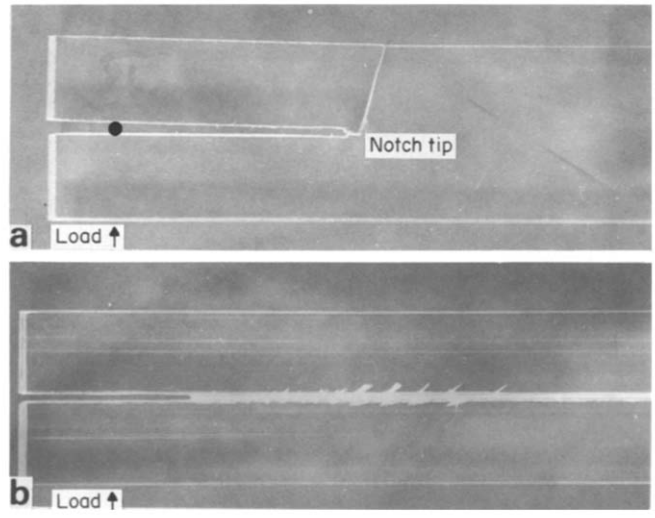

Figure 2 (a) ELS specimen after bending. (b) ELS specimen with side grooves after bending

Table 1 Energy release rate (G_{IIc}) of PMMA for mode II deformation of ELS specimens with various initial crack lengths (a_0) (length of specimen 100 mm, thickness 10 mm)

a_0 (mm)	G_{IIc} (J m^{-2})
20	355
25	510
30	476
40	436
50	403
60	434
Ave.	440 ± 40

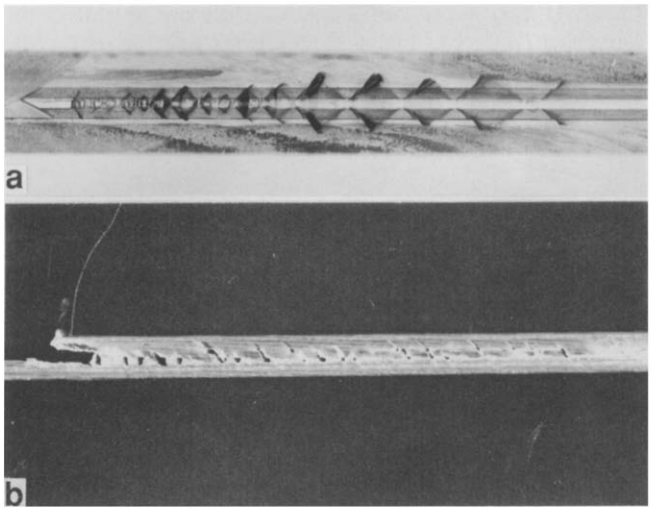

Figure 3 (a) Top view of the ELS specimen after bending. (b) Side view of crack tip in ELS specimen after bending

the compliance measured also for this type of specimen as mentioned above, critical energy release rates in the range:

$$7 < G_{IIc} < 10 \text{ kJ m}^{-2}$$

are obtained. These values are at least one order of magnitude higher than those for the crack opening mode. The remaining thickness between the side grooves of the originally 10 mm thick specimen had to be lower than 1.3 mm (mainly 1 mm was used), otherwise no shearing but again crack opening was observed. This need for very strong thinning of the failure plane by a factor of about 10 to get shearing supports the statement mentioned above that, under the macroscopic mode II condition, shear failure of a notch needs much more energy than crack opening, in our case more than an order of magnitude.

Figures 2b and *3* show the shearing fracture pattern of PMMA in more detail. The top and the side views reveal that before final fracture the crack tries to leave the shear plane (*Figures 3a* and *2b*) micromechanically by mode I crack opening at the beginning, but due to the thicker arms of the specimens outside the area between the side grooves the crack is forced to propagate mainly in the shear plane, at least for some length. The direction in which the crack wants to leave the shear plane in this side-grooved specimen is about $-40°$, thus lower than without side grooves. The stress field is obviously influenced by side grooves. Additionally the region in front of the crack tip is highly deformed (*Figure 3b*). The yield zone seems to be widely extended, showing also numerous cracks in the shear direction.

M-shaped specimen

The M-shaped specimen as described by Watkins[10], Brandt[11] and Jones[12] to measure mode II shear for ceramics and alloys is shown in *Figure 4* in the version used in this work. The central part of the specimen is pressed against the two outer rectangular pillars, with the consequence of shearing stress along the direction of both notches, which have been sharpened by tapping a razor blade into the notch. However, without side grooves the notch becomes unstable by an off-plane crack propagation (lower than $-70°$, *Figure 4a*), in spite of macroscopic compression stress at the notches. In this regard the failure situation at the main shear plane corresponds to the observations in shearing by tension. However, if the thickness of the shear plane was reduced with deep side grooves from 10 to 2 mm, shearing failure was provoked (*Figure 4b*). The compliance of this specimen can be described in the crack length region of interest by the linear expression (*Figure 5*):

$$C/C_0 = 1 + 0.0488(a - 3) \qquad (5)$$

(C_0 = compliance at the smallest possible crack length $a = 3$ mm, which is attainable in our specimen). From

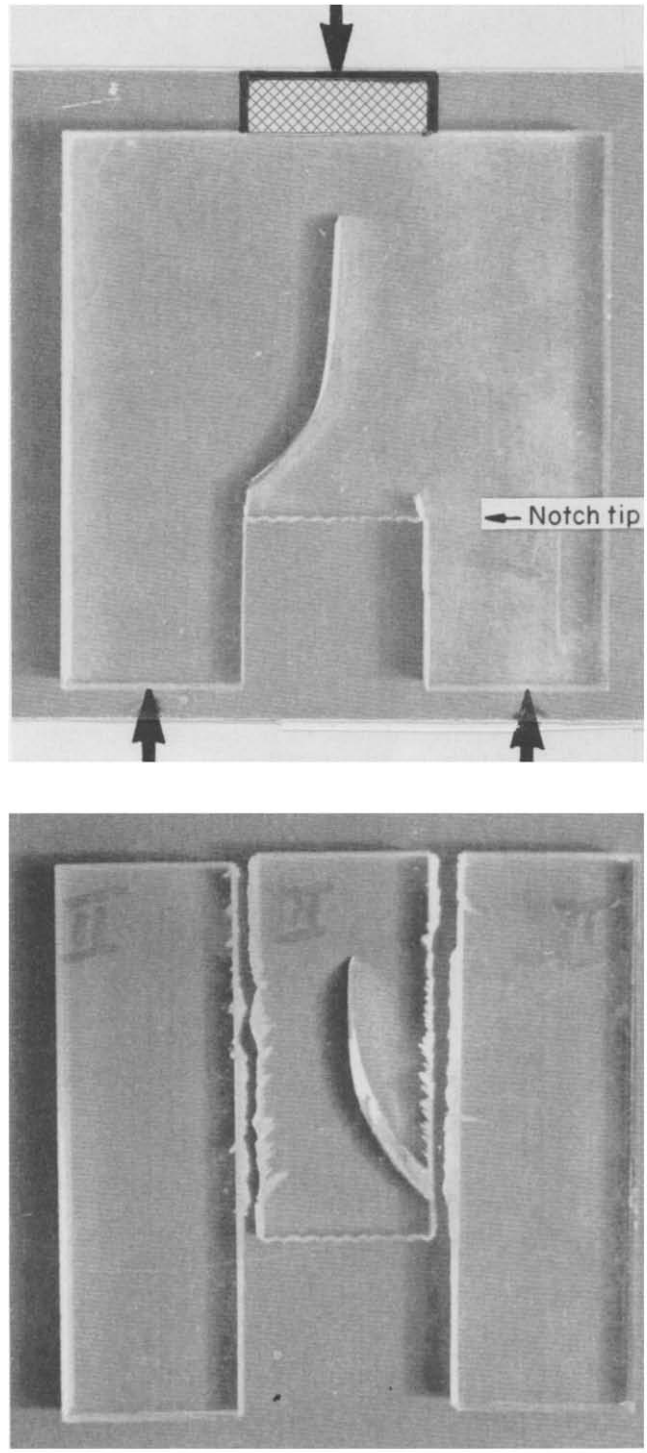

Figure 4 (a) M-shaped specimen after shear compression. (b) M-shaped specimen with side grooves after shear compression

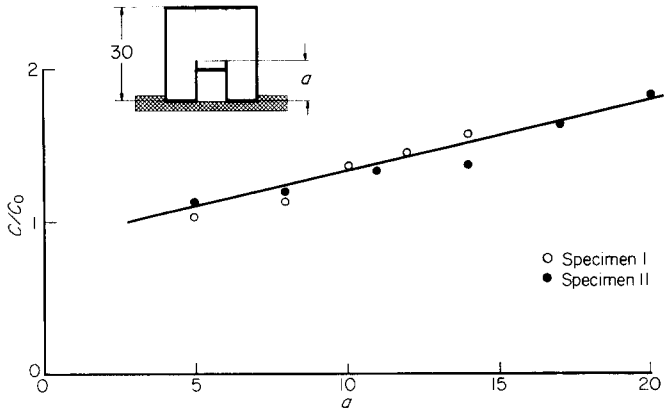

Figure 5 Compliance of M-shaped specimen with side grooves

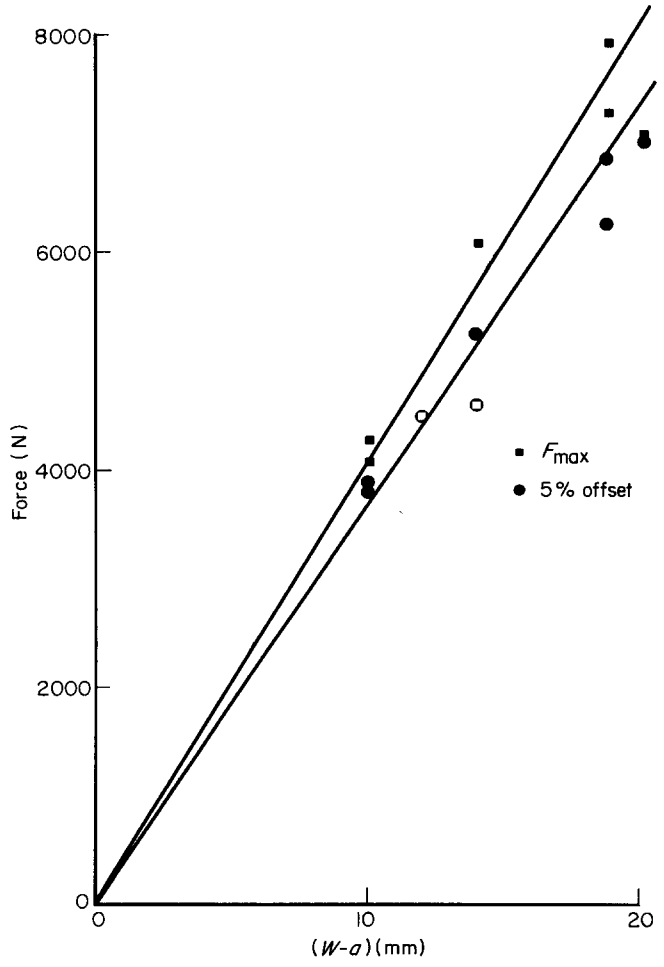

Figure 6 Failure strength (maximum stress or 5% offset values) of M-shaped specimens

equation (5) it follows that even in this case of shearing no fracture mechanics is applicable, since the differential coefficient of C according to equation (5) is independent of crack length and therefore no geometry-independent energy release rate G_{IIc} is attainable on the basis of equations (4) and (5). A plot (*Figure 6*) of the 5% offset value or of the maximum force as a function of the remaining part of the shear plane $(W - a)$ can be fitted by straight lines through the origin. From the slopes of these lines, failure shear strength according to:

$$\tau_f = \frac{1}{2B}\frac{dP}{d(W-a)} \qquad (6)$$

(B = width of the failure plane) is assessed. With the 5% offset values of the side-grooved specimens:

$$\tau_f \approx 62.2 \text{ N mm}^{-2}$$

is obtained, and by taking into account maximum stress at failure:

$$\tau_f \approx 67.7 \text{ N mm}^{-2} \qquad (7)$$

is calculated. The latter value is very close to the matrix shear strength τ_y as assessed on the basis of von Mises criterion from the tensile yield stress of PMMA (σ_y = 119 N mm^{-2}), from which follows:

$$\tau_y = \sigma_y/\sqrt{3} = 68.7 \text{ N mm}^{-2} \qquad (8)$$

Therefore, it seems that in contrast to Brandt's[11] claim of having measured the energy release rate G_{IIc} in sliding mode II of cementitious composites with this type of specimen, with polymers simply the matrix shear strength dominates the failure.

Prismatic specimens with inclined initial notches under uniaxial compression

By uniaxial compression of prismatic specimens as shown in *Figure 7* (insert), in which the initial notches are oblique to the compression direction, the notches again become unstable by an offset plane crack. However, if deep enough side grooves (in the present case at least one-third of the thickness) are milled along the plane of the initial notch, shear failure is observed. Irrespective of the overall shearing feature, the propagating crack wants to leave the shear plane, as can be seen in the side view of the specimen (*Figure 8*), where many small cracks oblique to the shear plane are discernible. The measured compliance for this type of specimen as a function of the length of the notch can be described for the specimen with 45° inclined initial notches by (*Figure 7*):

$$C/C_0 = 1.05 + 2.4(a/L)^3 \qquad (9)$$

With this compliance and equation (4) the energy release

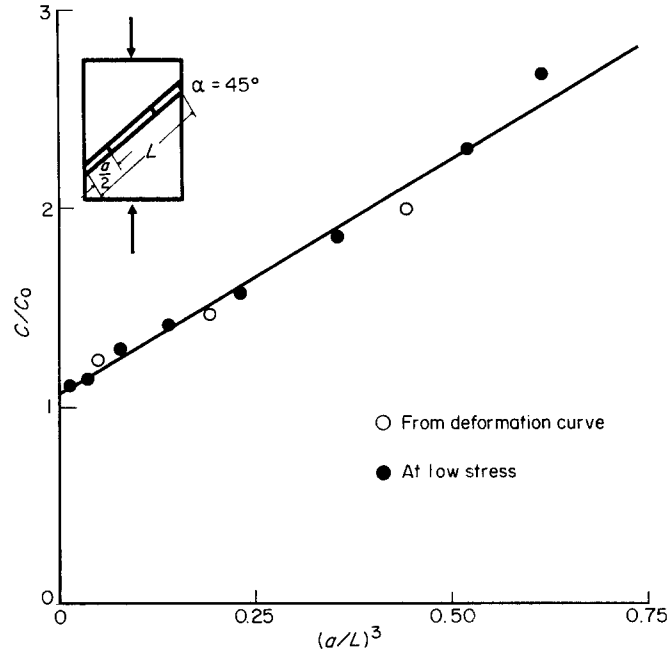

Figure 7 Compliance of side-grooved prismatic specimens with inclined initial notches

rates G_{IIc} as compiled in *Table 2* are evaluated from the 5% offset and maximum force values. The calculated G_{II} values are not independent of the geometry of the specimen. This deviation is in contrast to the fracture mechanics concept. If one tries to represent the failure strength alternatively by the criterion that matrix shear strength determines notch instability, the relationship:

$$\tau_f = (P \cos \theta)/B(W - a) \qquad (10)$$

is to be applied. The shear strengths, calculated in this way, are summarized in the last column of *Table 2*. It seems, indeed, that matrix shear strength describes the shear failure rather well. For 45° inclination with the higher friction between the crack surfaces, the 5% offset values correspond well to the matrix shear strength. For the steeper inclination of 30°, the maximum forces result in the matrix shear strength.

Looking through the transparent PMMA specimen on the shear plane of the side-grooved specimen, it is seen that small crazes or cracks are formed along the whole length of both side grooves (*Figure 9*) starting at the notch tips. As shown in *Figure 10* the fracture surface of PMMA after shearing is very rough and structured with deformation lines preferentially bowed in the shear direction. This rough surface resembles very strongly the widely documented 'hackle' structure[13] of the matrix in composites after having been fractured in mode II. It is to be assumed that in composites shearing of the matrix is enforced by the fibres, keeping the crack propagation in the shear plane. This constraint is very similar to the effect of side grooves. But in the case of fibres, crack opening is suppressed by fibres, not by a reduced shear plane. This effect of fibres can be demonstrated with a prototype for a SENB specimen, which consists of a sandwich structure with the following sequence of layers (*Figure 11*):

PMMA/carbon-fibre bundles/thin PMMA sheet/
carbon-fibre bundles/PMMA

The initial notch has been milled into the central PMMA sheet. By bending this bar, the crack front tries to leave its shear plane, as expected, and forms shell-shaped cracks between two fibre bundles (*Figure 11*). But if the density of the fibre bundles is high enough, then the

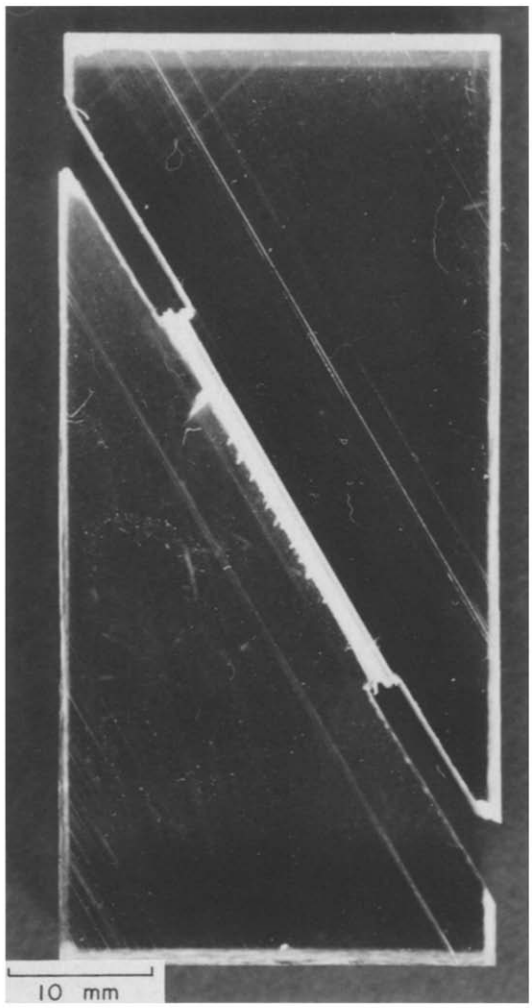

Figure 8 Shear failure in prismatic specimen with side grooves

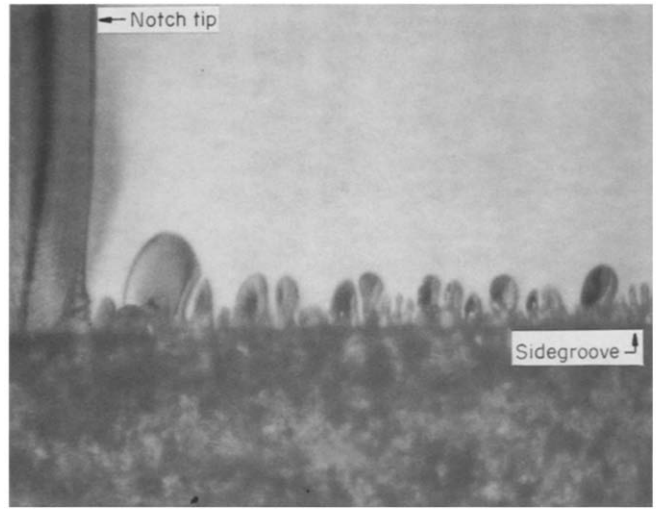

Figure 9 View of the deformed but not fractured shear plane of a side-grooved prismatic specimen

Table 2 Energy release rate (G_{IIc}) and shear yield stress (τ_f) of PMMA for mode II deformation of prismatic specimens with inclined (α) initial notches under uniaxial compression (a = length of notch, values calculated from 5% offset values and maximum failure strength)

α (deg)	a (mm)	G_{IIc} (5% offset) (kJ m^{-2})	G_{IIc} (P_{max}) (kJ m^{-2})	τ_f (5% offset) (N mm^{-2})	τ_f (P_{max}) (N mm^{-2})
45	18	24	30	71	81
	24	23	28	71	78
	32	13	13	68	80
30	18	14	17	63	70
	24	16	21	62	70
	31	18	23	61	69

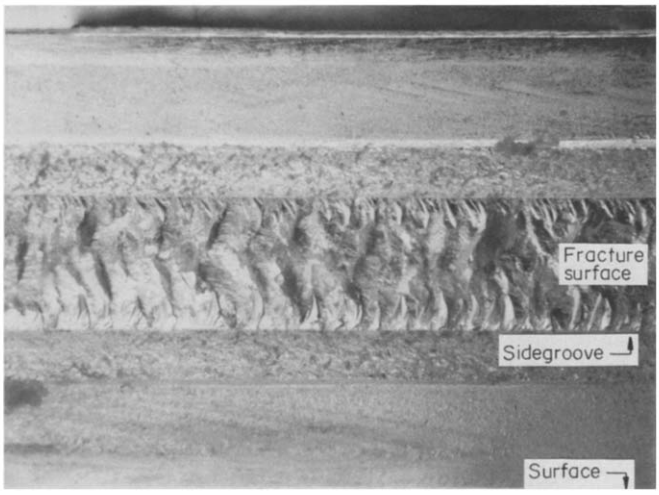

Figure 10 Fracture surface of prismatic specimen (side-grooved) after compression (30° inclination of initial notch)

extensive opening of the kinked crack under mode II condition is stopped, because fibres hinder further crack opening. But only this restriction due to fibres allows mode II shear failure in composites, as is measured in fracture mechanics.

CONCLUSIONS

When PMMA is stressed macroscopically in mode II to measure the mechanical properties in shear mode, this polymer fails microscopically by a mode I crack opening feature, and not by a sliding mode, as originally intended. Failure in shear must be enforced by reducing the area of the shear plane with respect to the rest of the material. This reduction can be realized with side grooves in the plane of the notch, but under this restriction failure turns out to be mainly given by the matrix shear strength, and not by a fracture mechanics defined sliding mode II. In composites, shear failure of the matrix is enforced by the fibres, which prevent crack opening on a macroscopic scale. As a consequence of these different failure mechanisms in pure and reinforced polymers, when deformed in mode II, the mechanical properties of composites are not expected to correlate in a simple way with G_{IIc} values of the matrix material alone.

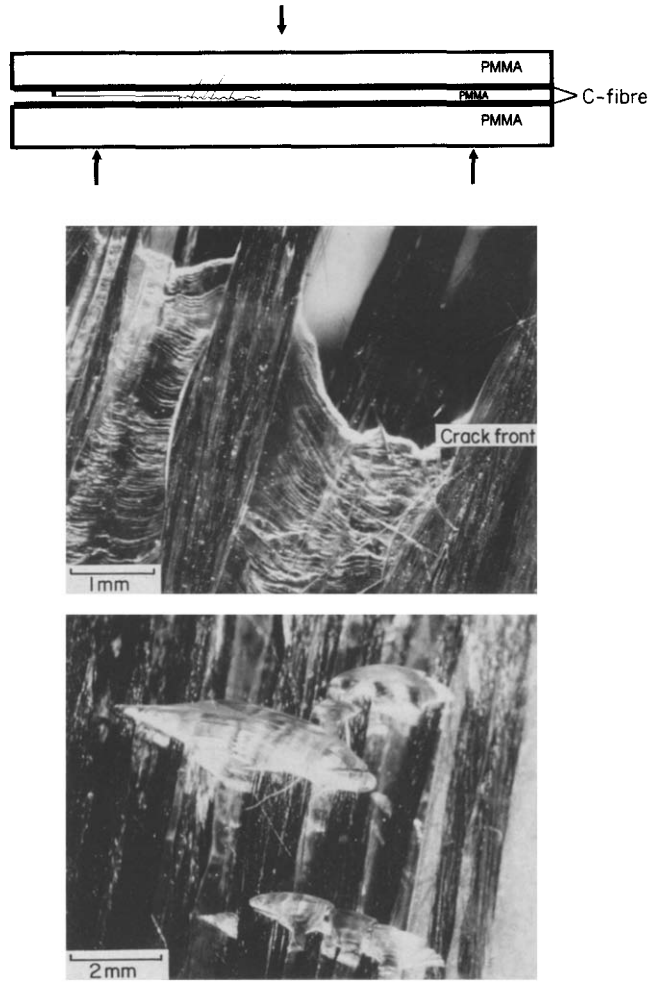

Figure 11 View of the shear plane of a sandwich-like structured carbon-fibre-reinforced PMMA specimen

REFERENCES

1 Richard, H. A., Tenhaeff, D. and Hahn, H. G. Int. Conf. and Exposition on Fatigue, Corrosion Cracking, Fracture Mechanics and Failure Analysis, Salt Lake City, Utah, 2–6 December 1985
2 Erdogan, F. and Sih, G. C. *J. Basic Eng.* 1963, December, 519
3 Sih, G. C. *Int. J. Fract.* 1974, **10**, 305
4 Buchholz, F. G. and Richard, H. A. Advances in Fracture Research, Proc. 7th Int. Conf. on Fracture (ICF7), Houston, Texas, 20–24 March 1989
5 Maji, A. K., Tasdemir, M. A. and Shah, S. P. *Eng. Fract. Mech.* 1991, **38**, 129
6 Maccagno, T. M. and Knott, J. F. *Eng. Fract. Mech.* 1989, **34**, 65
7 Williams, J. G. and Ewing, P. D. *Int. J. Fract. Mech.* 1972, **8**, 441
8 Ilcewicz, L. B., Keary, P. E. and Trostle, J. *Polym. Eng. Sci.* 1988, **28**, 592
9 Maiti, S. K. and Mahanty, D. K. *Eng. Fract. Mech.* 1990, **37**, 1251
10 Watkins, J. *Int. J. Fract.* 1983, **23**, R135
11 Brandt, A. M. and Prokopski, G. *J. Mater. Sci.* 1990, **25**, 3605
12 Jones, D. L. and Chrisholm, D. B. *Eng. Fract. Mech.* 1975, **7**, 261
13 Johannesson, T., Sjoblon, P. and Selden, R. *J. Mater. Sci.* 1984, **19**, 1171